Biochemical and Biophysical Research Communications 414 (2011) 192–198

Contents lists available at SciVerse ScienceDirect

Biochemical and Biophysical Research Communications

journal homepage: www.elsevier.com/locate/ybbrc

Label-free THz sensing of living body-related molecular binding using a metallic mesh

Takayuki Hasebe *, Yuki Yamada, Hitoshi Tabata

Department of Bioengineering, University of Tokyo, Bunkyo-ku, Tokyo 113-8656, Japan

ARTICLE INFO

Article history:
Received 9 September 2011
Available online 16 September 2011

Keywords:
Terahertz
Metallic mesh
Label-free
Sensing
FDTD simulations
PVDF membrane

ABSTRACT

We have demonstrated label-free THz sensing of living body-related molecular binding using a thin metallic mesh and a polyvinylidene difluoride (PVDF) membrane. Metallic meshes in the THz region are designed for anomalous transmission phenomena derived from a resonant excitation of surface waves. Additionally, they are designed to have a sharp dip in transmittance. The metallic mesh is very sensitive to a change of the refractive index of materials attached to the metallic mesh. In this paper, we report sensing of interactions between lectin and sugar using this technique. We found that the dip frequency shift, transmittance attenuation of the dip frequency, and peak shift of the derivative spectrum of the phase shift depend on the bonding amount of lectin–sugar interactions. We also applied this technique to detect avidin–biotin interactions, leading to the detection of a small amount of biotin (0.17 pg/mm^2).

1. Introduction

Terahertz (THz) wave technology is generally used in the frequency region from 0.1 to 10 THz. The terahertz wave is an energy domain that corresponds to the intermolecular vibration. Therefore, THz spectroscopy is suitable for the detection of biological macromolecules. The SPR method in the visible region cannot distinguish the specific binding and the nonspecific adsorption. On the other hand, THz sensing method has the possibility that the specific binding and the nonspecific adsorption can be distinguished. In the THz wave range, the refractive index and coefficient of absorptivity differ between single-stranded DNA and double-stranded DNA as determined by passive THz resonator devices based on planar waveguides [1]. The binding between biotin and avidin has been detected using double-modulated differential THz time-domain spectroscopy [2,3] and terahertz chemical microscope (TCM) [4]. Moreover, when the near field light of the terahertz wave is used, the entire cell can be measured, because the wavelength of the terahertz wave is hundreds of microns.

Metallic meshes with a periodic grid have been employed in the micro and the THz wave region [5,6], and they have a frequency domain in which the transmittance increases resonantly [7,8]. This is known as an anomalous transmittance phenomenon that is strongly enhanced when incident waves are resonantly matched with surface waves excited on the metallic surface [9]. In addition, the metallic mesh produces a sharp dip structure due to an obliquely incident element [10]. The sharp dip structure is very sensitive to a small change of the refractive index on the metallic surface [11]. Therefore, label-free detection of small amounts of proteins has been achieved using the metallic mesh [12]. Furthermore, THz sensing of the uniting of biotin and avidin by a metallic mesh technique has been reported [13]. However, quantitative estimation of interactions between bio-molecules (e.g., estimation of the binding constant) has not been reported until now in THz wave region. On the other hand, the metallic mesh can provide a sensing area in two dimensions. Terahertz sensing in two dimensions of thin poly(ethylene terephthalate) film thickness using a metallic mesh has been reported [14]. Moreover, terahertz sensing in two dimensions using the metallic mesh can be used in microarray technology.

Microarray technology [15] is expected to be used as a tool for high throughput in drug development and life sciences because the simultaneous detection of tens of thousands of spots and an inclusive analysis of the interaction of various biological materials becomes possible. However, the labeling procedure is complex and takes time, and labeling materials causes a reactive influence such as steric hindrance, etc. Therefore, it is hoped that label-free detection will solve these problems.

A sugar chain is the third chained life-giving molecule following DNA and protein. The sugar chain covers all the surface of the cells of a living organism including humans, and takes part in various bodily functions such as intercellular interactions, foreign body recognition, etc. Over one million kinds of sugar chains are known,

* Corresponding author. Address: Department of Bioengineering Engineering, University of Tokyo, 2-11-16 Yayoi, Bunkyo-ku, Tokyo 113-0032, Japan. Fax: +81 3 5841 1870.
E-mail address: tt097216@mail.ecc.u-tokyo.ac.jp (T. Hasebe).

0006-291X/$ - see front matter © 2011 Elsevier Inc. All rights reserved.
doi:10.1016/j.bbrc.2011.09.055

and a suitable sugar chain analysis technology is needed. A lectin is a protein showing compatibility with the sugar chain. Depending on the kind of lectin, the structural feature of the part that unites with the sugar chain is different (e.g., the extent of branching, the linking mode, and presence of the terminal modification). By evaluating the connectivity with tens of different kinds of lectin in the microarray, the sugar chain structure of a sample can be estimated roughly. Recent lectin microarray technology has been utilized for a variety of medical applications such as the search for a new tumor marker, early diagnostics of cancer and infectious disease, as well as the rapid screening of stem cells used for regenerative medicine. However, the binding force of lectin–sugar chain interactions is weaker than the binding force of biotin–avidin and antigen–antibody reactions. The binding constants of biotin–avidin and antigen–antibody reactions are $10^{14}\,M^{-1}$ and 10^{7}–$10^{9}\,M^{-1}$, respectively. On the other hand, the lectin–sugar chain interaction has a small binding constant of 10^{3}–$10^{5}\,M^{-1}$ [16]. It is thought that optical properties in the THz region include weak chemical characters such as the hydrogen bond, van der Waals force and hydrophobic interactions. Binding in the lectin–sugar chain interaction is caused by the hydrogen bond, van der Waals force, hydrophobic interactions, etc. Therefore, THz spectroscopy is one of the candidate methods for observation and analysis of lectin–sugar chain interactions. Qualitative measurement of lectin–sugar chain interactions by label-free THz sensing using the metallic mesh and the polyvinylidene difluoride (PVDF) membrane is regarded as a promising approach for the lectin microarray. THz waves easily penetrate the PVDF membrane.

In this paper, we report label-free THz sensing of the lectin–sugar interaction using the metallic mesh and the PVDF membrane with quantitative and qualitative analysis. We determine the small binding constant of the lectin–sugar interaction. Furthermore, we report the detection of a small amount of biotin, as confirmed from investigations of the binding between biotin and avidin.

2. Materials and methods

2.1. Transmission characteristics of the metallic mesh

A schematic representation of the structure of the metallic mesh is shown in Fig. 1A. Transmission properties of the metallic mesh markedly depend on the size and cycle of the opening holes [17,18]. The wavelength (λ_p) of the anomalous transmittance peak can be calculated by the following expression with a grating period (g) [17]:

$$\lambda_p = 1.15g \tag{1}$$

On the other hand, the wavelength (λ_d) of the dip peak can be written as [10]:

$$\lambda_d = 1.73g - 1.435b \tag{2}$$

where b is the length of the metallic portion. In this work, we use nickel mesh fabricated by electroforming processing with g, b, and t values of 302, 74, and 6 μm, respectively. A transmission spectrum of the metallic mesh at an incident angle of 0° is shown in Fig. 1B, revealing that λ_p and λ_d were 0.72 and 0.86 THz, respectively. These frequencies are designed so as not to overlap frequencies of the rotation transition of water vapor. The anomalous transmission phenomenon of the metallic mesh is based on a uniting and re-radiation with a surface wave by a mode-like surface plasmon polariton [19]. The resonant frequency (f_{sw}) of the surface wave is described as follows [17,20]:

$$f_{sw} = |k_{in} + G|\frac{c}{2\pi}\sqrt{\frac{\varepsilon_m + \varepsilon_d}{\varepsilon_m \varepsilon_d}} \tag{3}$$

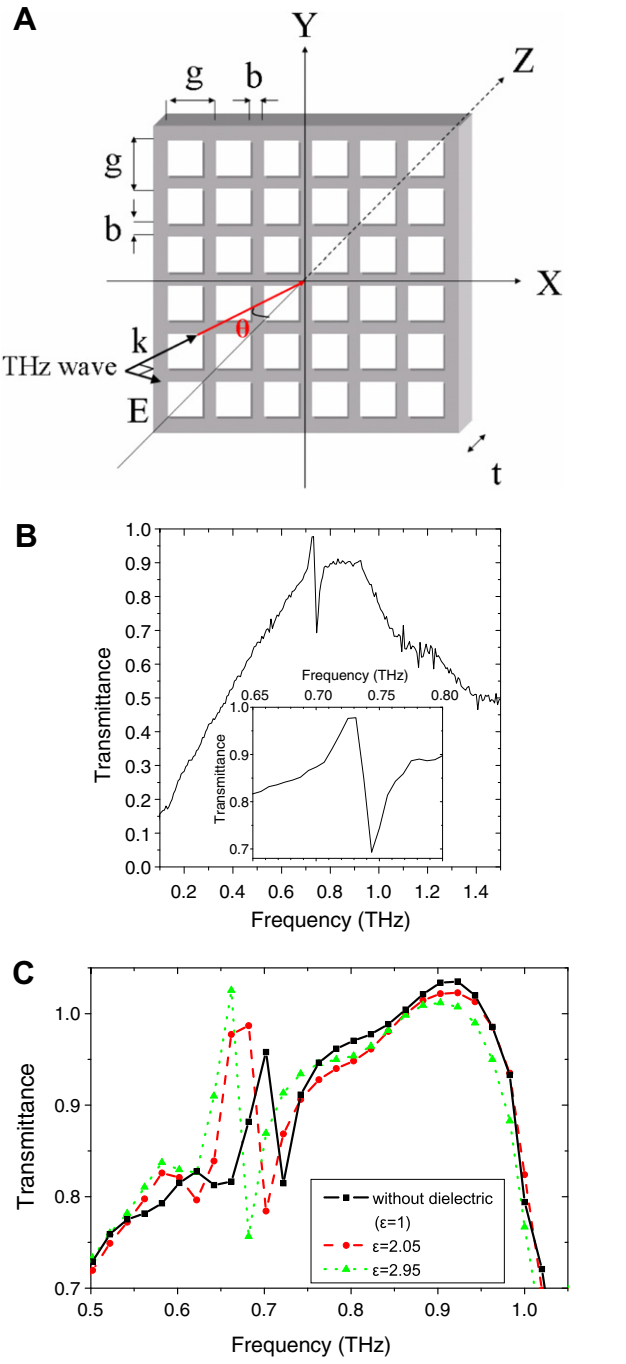

Fig. 1. (A) Schematic representation of the structure of the metallic mesh. (B) The transmission spectrum in the THz region of the metallic mesh with g, b and t values of 302, 74 and 6 μm in the vertically incident region, respectively. (C) The dielectric constant dependence of the transmission spectrum of the metallic mesh attached to the dielectric film in FDTD simulations.

where k_{in} is the in-plane wave vector of the incident THz wave, G is the reciprocal lattice vector of the periodic structure, and ε_m and ε_d are dielectric constants of the metal and the measured material, respectively. f_{sw} changes according to the density and refractive index of the measured material [21]. A dip structure appears in the anomalous transmission region by an obliquely incident element [10,22]. THz pulses are converged onto a sample by off-axis parabolic mirrors. Therefore, an obliquely incident element is produced even at an incident angle of 0°. Furthermore, it is reported that the dip frequency is sensitive to the density and refractive index of the measured material [12].

2.2. Experimental setup

In this work, all samples were measured using THz time-domain spectroscopy (THz–TDS) [23]. A laser (λ = 780 nm) with a pulse width of 85 fs is split into a pump and a probe beam with a repetition rate of 50 MHz. The chopped pump beam is focused on a photoconductive dipole antenna (low temperature growth(LT)-GaAs) to generate THz pulses on the basis of ultrafast transport charged carriers. The THz pulses propagate through four off-axis parabolic mirrors, and are focused onto the photoconductive dipole antenna (LT-GaAs). The detection signal is amplified with a current amplifier, and it is synchronously demodulated with a lock-in amplifier. By delaying the timing of the probe pulse to the pump pulse, a waveform for an electromagnetic pulse is obtained. Metallic meshes are made using electroforming by Taiyo Industrial Co. Ltd.

2.3. Dielectric constant dependence on transmission characteristics of the metallic mesh

We evaluated the dielectric constant dependence of the transmission spectrum of the metallic mesh attached to the dielectric film using finite difference time domain (FDTD) simulations [24]. The incident wave was an impulse *p*-polarized plane wave, as shown in Fig. 1A. We used a nickel mesh and FDTD simulations with *g*, *b*, *t*, and θ values of 302, 74, 6 μm, and 7°, respectively. The thickness of the dielectric film was a constant 3 μm. The dielectric constant of the dielectric film was changed to 2.05, 2.95, and 1 (without the dielectric film). The boundary condition of *X* axis and *Z* axis is used the absorbing boundary condition of Mur of one dimension, and the boundary condition of *Y* axis is used a periodic boundary condition [24]. We calculated the transmission properties using a Fourier transform.

2.4. Label-free THz sensing of the lectin–sugar interaction

Samples were prepared according to the following procedure. A hydrophobic PVDF membrane was soaked in a 50 μM lectin solution for one hour. Concanavalin-A (Con-A) was used for lectin. Fixation of Con-A on the membrane was performed by soaking in a 2.5% glutaraldehyde solution for ten minutes. After washing three times with ultrapure water for five minutes, the Con-A fixed on the membrane was soaked in a D(+)-Glucose (Glc) solution at 5, 10, 50 and 100 mM for one hour, and then was washed with ultrapure water for 5 min. The membrane was dried sufficiently. The membrane was finally attached firmly to the metallic mesh with holding between two aperture plates tightening screws. In this measurement, samples were measured with an incident angle of 7° using THz–TDS.

2.5. Qualitative analysis of the lectin–sugar interaction

Sample preparation is explained in a manner similar to the Chapter 4.2. Con-A 20 μM solution was used for lectin solution. D(+)-Glucose (Glc), D(+)-Mannose (Man), N-Acetyl-D(+)-glucosamine (GlcNAc), and D(+)-Galactose (Gal) 10 mM solution were used for the monosaccharide solution. In this measurement, samples were measured with an incident angle of 7° using THz–TDS.

2.6. High sensitivity detection of the biotin–avidin reaction

Molecules of 4′-hydroxyazobenzene-2-carboxylic acid (HABA) exhibit weak binding with avidin. The HABA/avidin complex has an absorption peak at 500 nm, which decreases by replacing biotin with the HABA through the HAVA/avidin complex. The HABA substitution method is used to estimate the biotin labeling index of protein. A HABA/avidin assay mixture (900 μL) was added to a biotin solution (100 μL) at various concentrations from 0 to 100 μM. At first, we confirmed the chemical reaction between avidin and biotin by absorbance spectra of visible range in a different biotin concentration. Absorbance spectra of obtained samples was measured using a UV/Vis/NIR spectrometer with a cell length of 1.8 mm. The samples (2 μL) were then put on a side of the membrane in a square shape of about 1 cm. The liquid drop extended 6 mm in diameter. The membrane was dried for at least 2 h. The membrane was finally attached firmly to the metallic mesh with holding between two aperture plates tightening screws. In this measurement, samples were measured with an incident angle of 7° using THz–TDS.

3. Results and discussion

3.1. Dielectric constant dependence on transmission characteristics of the metallic mesh

The dielectric constant dependence of the transmission spectrum of the metallic mesh attached to the dielectric film in FDTD simulations is shown in Fig. 1C. The dip frequency gradually shifted to a low frequency when the dielectric constant of the dielectric film was increased. In addition, the peak of the anomalous transmission range at 0.92 THz decreased in response to an increase of the dielectric constant of the dielectric film. These results indicate that the change of the dielectric constant of the dielectric film can be detected by the change in transmission characteristics of the metallic mesh. These results can be applied to the sensing of living body-related molecular binding. The sensing of living body-related molecular binding is possible by the frequency shift of the dip and the transmittance change of the anomalous transmittance peak.

In the sensing by the shift of the dip frequency, the sensitivity of the change of the dielectric constant is 0.0335/GHz in FDTD simulations. If a THz wave measurement system with a high frequency resolution can be used, a minute change of the dielectric constant can be obtained. For example, THz wave generation technology using a photomixer and Uni-Traveling-Carrier Photodiode (UTC-PD) has a high frequency resolution in the kHz range [25].

3.2. Label-free THz sensing of the lectin–sugar interaction

Transmittance spectra in the vicinity of the dip frequency are shown in Fig. 2A. Glc concentration (Glc) was systematically changed to 5, 10, 50 and 100 mM under a constant Con-A concentration. The dip frequency and transmittance attenuation was dependent on (Glc) (Fig. 2B). The dip position shifted gradually to a low frequency when (Glc) increased. This result is similar to the FDTD simulation result in Fig. 1C. The frequency shift (Δf_{dip}) of the dip position was 6.3, 12.5, 18.8 and 25.0 GHz at a (Glc) of 5, 10, 50 and 100 mM, respectively. On the other hand, attenuation of transmittance was 0.027, 0.057, 0.118 and 0.096 at a (Glc) of 5, 10, 50 and 100 mM, respectively. These results indicated generation of an interaction between lectin and sugar, which should be related to a change of the refractive index of the membrane caused by the uniting of Con-A and glucose.

Derivative spectra of the phase shift experimentally obtained in the vicinity of the dip frequency are shown in Fig. 2C. The peak shift (Δf_{der}) of derivative spectra is also shown in Fig. 2D. The peak frequency of derivative spectra systematically shifted to a low frequency with increasing (Glc). Δf_{der} was 12.2, 12.2, 18.3 and 24.4 GHz at a (Glc) of 5, 10, 50 and 100 mM, respectively, indicating that the derivative spectra include information concerning the interaction between lectin and sugar.

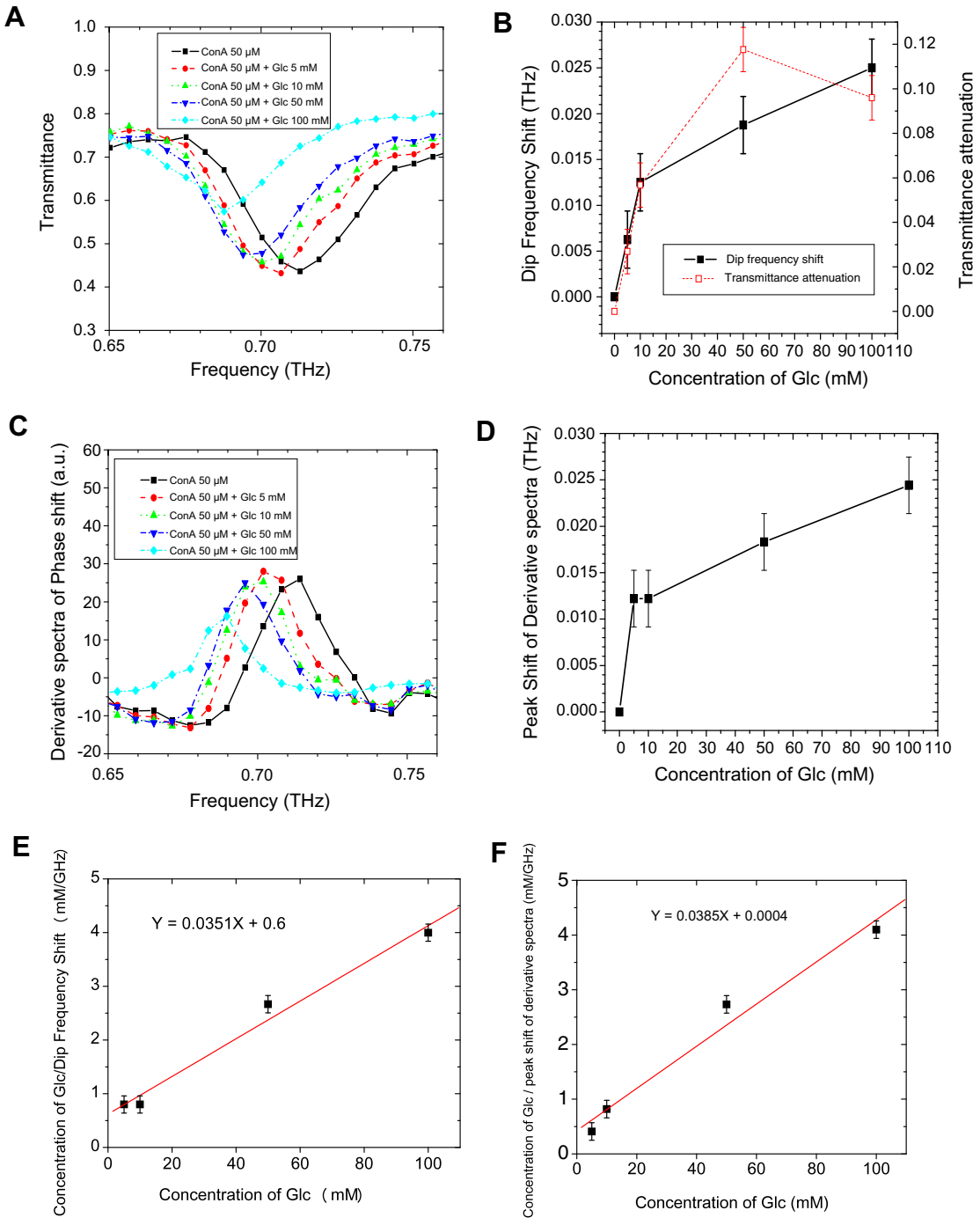

Fig. 2. THz sensing of binding between Con-A and Glc using the metallic mesh and the membrane. The Glc concentration was 5, 10 and 50 × 10^{-3} M with a constant Con-A solution concentration of 5 × 10^{-5} M. (A) Transmission spectra of samples with binding between Con-A and Glc on the metallic mesh. (B) Dependence of the dip frequency shift and transmittance attenuation of the dip frequency on Glc concentration. (C) Derivative spectra of the phase shift. (D) The peak shift of derivative spectra of the phase shift. (E) The correlation between (Glc) and (Glc)/Δm obtained from the dip frequency shift. (F) The correlation between (Glc) and (Glc)/Δm obtained from the peak shift of derivative spectra of the phase shift.

The binding constant (K_b) between Con-A and glucose molecules can be estimated as follows [26]:

$$\frac{(\mathrm{Glc})}{\Delta m} = \frac{(\mathrm{Glc})}{\Delta m_{\max}} + \frac{1}{\Delta m_{\max} K_b} \tag{4}$$

where Δm and $\Delta m_{\max}$ are the binding amount and maximum binding amount, respectively. Here, we assume that the value of Δf_{dip} is proportional to that of Δm. The correlation between (Glc) and (Glc)/Δm obtained from Δf_{dip} is given in Fig. 2E. The values of $\Delta m_{\max}$ and K_b were approximately 28.5 GHz and 100 M^{-1}, respectively, as calculated from a slope and intercept in Fig. 2E. The correlation between (Glc) and (Glc)/Δm obtained from Δf_{der} is given in Fig. 2F. From Fig. 2F, the values of $\Delta m_{\max}$ and K_b were about 26.0 GHz and 100 M^{-1}, respectively. Experimental values of K_b are not in good agreement with a previously reported value (600 M^{-1}) [27]. If chemical processing on the PVDF membrane is optimized, it will approach the previously reported value (600 M^{-1}). The sensitivity of glucose is 0.8 mM/GHz in the low concentration range. The fre-

quency resolution of this THz wave measurement system is 6.25 GHz. If a THz wave measurement system with a high frequency resolution can be used such as THz wave generation technology using a photomixer and UTC-PD, the binding constant can be obtained more accurately.

3.3. Qualitative analysis of the lectin–sugar interaction

Transmittance spectra of samples with a different monosaccharide type are shown in Fig. 3A comprising 10 mM of Glc, Man, GlcNAc and Gal, with a Con-A solution concentration of 20 μM. Δf_{dip} and transmittance attenuation was associated with the monosaccharide solution types (Fig. 3B). The dip frequency shifted to a low frequency when Con-A was united with Glc and Man. This result is similar to the FDTD simulation result in Fig. 1C. The same Δf_{dip} value of 6.3 GHz was observed for Glc and Man concentrations of 10 mM, and we could not observe any frequency shift when GlcNAc and Gal were used as a monosaccharide. Furthermore, we found that transmittance attenuation increased when Glc and Man was united for Con-A. In contrast, a clear change of transmittance attenuation was not seen in cases of GlcNAc and Gal. This is due to the fact that because Con-A does not combine with GlcNAc and Gal, GlcNAc and Gal are flushed from the membrane after washing. The change of Δf_{dip} should be based on the refractive index of the membrane. From Eq. (3), the value of f_{sw} is dependent on a change of ε_d, which is reflected by a dip frequency shift, indicating that the interaction between lectin and sugar was measured by the peak shift of the dip frequency. The derivative spectra of the phase shift and its peak shift (Δf_{der}) are shown in Fig. 3C and D. The peak position in derivative spectra moved to a low frequency as Con-A united with Glc and Man. Δf_{der} showed the same value of 6.1 GHz in the case of both Glc and Man. In contrast, we could not obtain any peak shift when GlcNAc and Gal were used.

The above result indicates that label-free THz sensing using the metallic mesh and the PVDF membrane can detect a peculiar reaction between lectin and sugar. Qualitative THz sensing of the lectin–sugar chain interaction using the metallic mesh and the membrane is expected to be used for the lectin microarray. The metallic mesh can provide a sensing area in two dimensions. Moreover, since the wavelengths of a terahertz wave are hundreds of microns in size, a sufficient spatial resolution is obtained in imaging of the microarray.

3.4. High sensitivity detection of the biotin–avidin reaction

Difference absorbance spectra in the visible region of avidin/HABA-biotin are shown in Fig. 4A with a biotin weight per unit area of 4.4, 22, 44, 220, 352, 440 and 4400 pg/mm^2 (0.01, 0.05, 0.1, 0.5, 0.8, 1, and 10 μM). Difference in absorbance intensities gradually enhanced when the biotin concentration increased. The HABA/avidin complex gives strong absorption at 500 nm since the affinity between HABA and avidin is relatively weak (dissociation constant: $K_d = 5.8 \times 10^{-6}$ M) compared to the affinity between biotin and avidin ($K_d = 1 \times 10^{-15}$ M). Biotin can easily replace HABA from the HABA/avidin complex, resulting in a decrease of the absorption at 500 nm. Fig. 4A indicates that the difference absorbance of 500 nm was enhanced when the level of biotin exceeded 44 pg/mm^2 (0.1 μM).

Transmission spectra in the THz region of the avidin/biotin complex on the metallic mesh are shown in Fig. 4B. A systematic change was observed in the frequency region from 0.5 to 1.0 THz, originating from the anomalous transmission. The transmittance change at 0.775 THz with a biotin weight per unit area of 0.17, 1.7, 17 and 170 pg/mm^2 (0.01, 0.1, 1, and 10 μM) is shown in Fig. 4C. The frequency of 0.775 THz corresponds to a peak of the anomalous transmission band. The peak of the anomalous transmission band decreased in response to a biotin amount from 0 to 170 pg/mm^2 due to HABA/avidin–biotin reactions. This result is similar to the FDTD simulation result in Fig. 1C. As a comparative experiment, we measured transmission spectra of the membrane on which were placed 2 μL of solution of the avidin/biotin complex

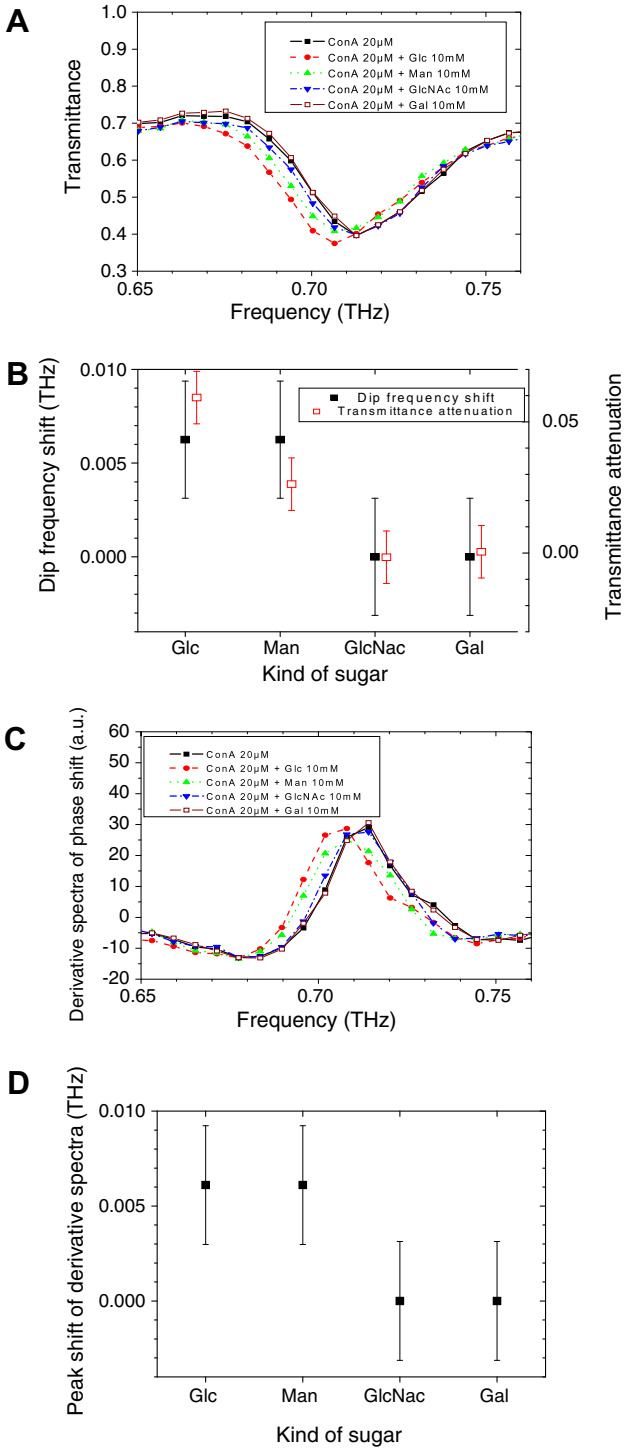

Fig. 3. (A) Transmittance spectra of samples with different monosaccharide type comprising 10 mM of glucose, Man, GlcNAc and Gal, with a Con-A solution concentration of 20 μM. (B) The dip frequency shift and transmittance attenuation of the dip frequency. (C) Derivative spectra of samples with different monosaccharide type comprising 10 mM of glucose, Man, GlcNAc and Gal, with a Con-A solution concentration of 20 μM. (D) The peak shift obtained from the derivative spectra of the phase shift.

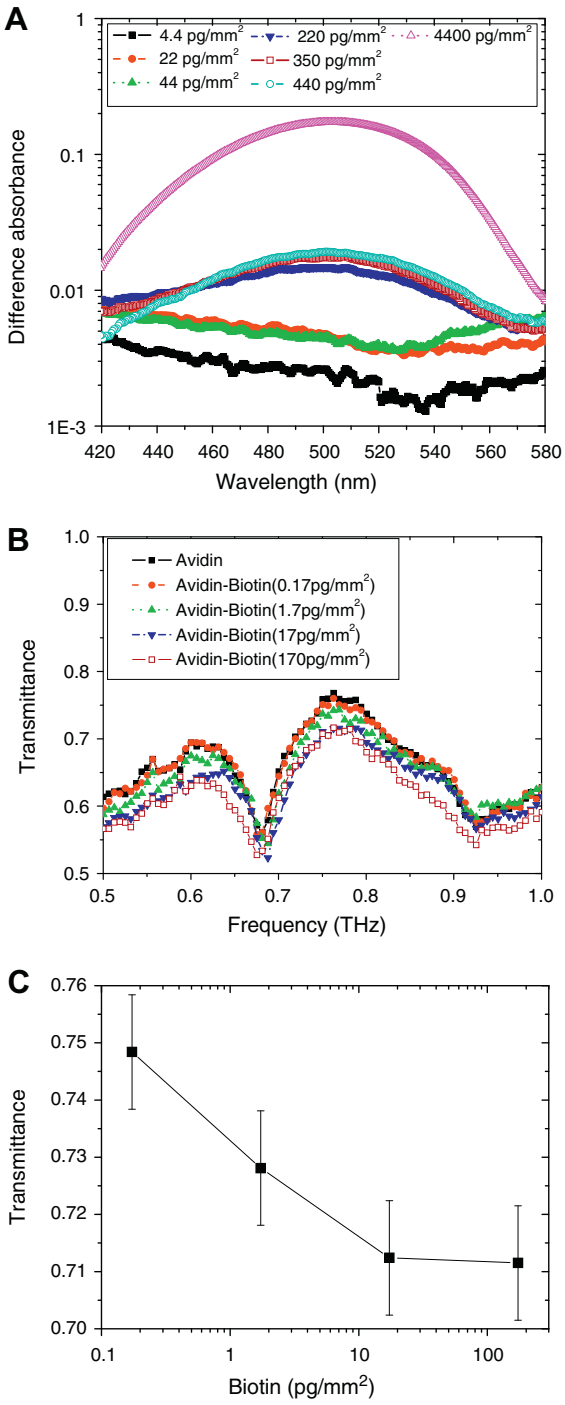

Fig. 4. (A) Difference absorbance spectra of the avidin/HABA-biotin reaction with a biotin amount from 4.4 to 4400 pg/mm^2. (B) THz transmission spectra of the membrane using the metallic mesh with 2 μl of solution of the avidin/biotin complex with a biotin amount of 0.17, 1.7, 17, and 170 pg/mm^2. (C) Transmittance at 0.775 THz with a biotin amount of 0.17, 1.7, 17, and 170 pg/mm^2.

without the metallic mesh. However, a systematic change was not observed. A change in transmittance was not induced even with a large biotin amount of 170 pg/mm^2.

We also examined whether a decrease of the transmittance was caused by the increase of biotin concentration. THz transmittance spectrum of the biotin pellet is measured. Feature peaks are derived from biotin, and do not produce a change of the anomaly transmission because these peaks do not extend to broad bands. As another comparative experiment, we measured transmittance spectra of the biotin placed only on the membrane, which was attached firmly to the metallic mesh with holding between two aperture plates tightening screws. We could not confirm a systematic change of the transmittance intensity. Since biotin is a small molecule, the change of the THz spectrum is very small only for the biotin molecule.

The above result indicates that a decrease of the transmittance intensity is closely associated with binding in the avidin–biotin reaction, which allowed us to detect a small biotin amount of 0.17 pg/mm^2. Our results indicated a higher sensitivity than that associated with previously reported techniques such as double-modulated differential THz–TDS (biotin 1 ng/mm^2) [2] (avidin 103 pg/mm^2) [3], the interference effect of terahertz (biotin 27 ng/mm^2) [28], and other research related to a metallic mesh (biotin 650 pg/mm^2) [13]. To achieve a high sensitivity, it is necessary to firmly attach the membrane to the metallic mesh. In our experiment, the membrane is firmly and strongly attached to the metallic mesh mechanically.

Acknowledgment

This work was supported by the National Agriculture and Food Research Organization (NARO).

References

[1] M. Nagel, P.H. Bolivar, M. Brucherseifer, H. Kruz, A. Bosserhoff, R. Buttner, Integrated THz technology for label-free genetic diagnostics, Appl. Phys. Lett. 80 (2002) 154.
[2] S.P. Mickan, A. Menikh, H. Liu, C.A. Mannella, R. MacColl, D. Abbott, J. Munch, X.-C. Zhang, Label-free bioaffinity detection using terahertz technology, Phys. Med. Biol. 47 (2002) 3789.
[3] A. Menikha, S.P. Mickan, H. Liu, R. MacColl, X.-C. Zhang, Label-free amplified bioaffinity detection using terahertz wave technology, Biosens. Bioelect. 20 (2004) 658.
[4] T. Kiwa, Y. Kondo, Y. Minami, I. Kawayama, M. Tonouchi, K. Tsukada, Terahertz chemical microscope for label-free detection of protein complex, Appl. Phys. Lett. 96 (2010) 211114.
[5] W. Culshaw, Reflectors for a microwave Fabry-Perot interferometer, IEEE Trans. Microwave Theory Tech. MTT-7 (1959) 221.
[6] K. Sakai, T. Fukui, Y. Tsunawaki, H. Yoshinaga, Metallic Mesh Bandpass Filters and Fabry-Perot Interferometer for the Far Infrared, Jpn. J. Appl. Phys. 8 (1969) 1046.
[7] R. Ulrich, K.F. Renk, L. Genzel, Tunable submillimeter interferometers of the Fabry-Perot type, IEEE Trans. Microwave Theory Tech. MTT-11 (1963) 363.
[8] R. Ulrich, Far-infrared properties of metallic mesh and its complementary structure, Infrared Phys. 7 (1967) 37.
[9] T.W. Ebbesen, P.A. Wolff, Extraordinary optical transmission through sub-wavelength hole arrays, Nature 391 (1998) 667.
[10] J.M. Lamarre, M. Charra, Metallic mesh properties and design of submillimeter filters, Int. J. Infrared Millimeter Waves 2 (1981) 273.
[11] M. Tanaka, F. Miyamaru, M. Hangyo, T. Tanaka, M. Akazawa, E. Sano, Effect of a thin dielectric layer on terahertz transmission characteristics for metal hole arrays, Opt. Lett. 30 (2005) 1210.
[12] H. Yoshida, Y. Ogawa, Y. Kawai, S. Hayashi, A. Hayashi, C. Otani, E. Kato, F. Miyamaru, K. Kawase, Terahertz sensing method for protein detection using a thin metallic mesh, Appl. Phys. Lett. 91 (2007) 253901.
[13] H. Yoshida, Y. Kawai, S. Hayashi, Y. Ogawa, Label-free detection of protein using a metallic mesh, IEICE Tech. Rep. ED2007-205 (2007-11) (in Japanese).
[14] S. Yoshida, E. Kato, Y. Nakagomi, Y. Ogawa, K. Kawase, Terahertz sensing of thin poly(ethylene terephthalate) film thickness using a metallic mesh, Appl. Phys. Express 2 (2009) 012301.
[15] H.-J. Mueller, T. Roeder (Eds.), Microarrays, Elsevier Academic Press, 2006.
[16] Y. Kobayashi, H. Kawagishi, Sugar-binding protein lectin, Bio Industry 27 (2010) 6.
[17] F. Miyamaru, M. Tanaka, M. Hangyo, Effect of hole diameter on terahertz surface-wave excitation in metal-hole arrays, Phys. Rev. B 74 (2006) 153416.
[18] C.-C. Chen, Transmission of microwave through perforated flat plates of finite thickness, IEEE Trans. Microwave Theory Technol. 21 (1973) 1.
[19] H.F. Ghaemi, T. Thio, D.E. Grupp, T.W. Ebbesen, H.J. Lezec, Surface plasmons enhance optical transmission through subwavelength holes, Phys. Rev. B 58 (1998) 6779.
[20] H. Reather, Surface Plasmons on Smooth and Rough Surfaces and on Gratings, Springer-Verlag, Berlin, 1988.
[21] F. Miyamaru, S. Hayashi, C. Otani, K. Kawase, Y. Ogawa, H. Yoshida, E. Kato, Terahertz surface-wave resonant sensor with a metal hole array, Opt. Lett. 31 (2006) 1118.

[22] S. Yoshida, K. Suizu, E. Kato, Y. Nakagomi, Y. Ogawa, K. Kawase, A high-sensitivity terahertz sensing method using a metallic mesh with unique transmission properties, J. Mol. Spectrosc. 256 (2009) 146.

[23] Y.-S. Lee (Ed.), Principles of Terahertz Science and Technology, Springer, 2008.

[24] A. Taflove, S.C. Hangness (Eds.), Computational Electrodynamics the Finite-Difference Time-Domain Method, Artech House, Boston, 1995.

[25] N. Shimizu, H.-J. Song, Y. Kado, T. Furuta, A. Wakatsuki, Y. Muramoto, NTT GIJUTU Journal 12 (2008) 37 (in Japanese).

[26] T. Sato, T. Serizawa, F. Ohtake, M. Nakamura, T. Terabayashi, Y. Kawanishi, Y. Okahata, Quantitative measurements of the interaction between monosialoganglioside monolayers and wheat germ agglutinin (WGA) by a quartz-crystal microbalance, Biochim. Biophys. Acta 1380 (1998) 82.

[27] M. Ambrosi, N.R. Cameron, B.G. Davis, Lectins: tools for the molecular understanding of the glycocode, Org. Biomol. Chem. 3 (2005) 1593.

[28] Y. Ogawa, S. Hayashi, M. Oikawa, C. Otani, K. Kawase, Interference terahertz label-free imaging for protein detection on a membrane, Opt. Express 16 (2008) 22083.